

# Ion bombardment induced smoothing of amorphous metallic surfaces: Experiments versus computer simulations

Sebastian Vauth\* and S. G. Mayr†

*I. Physikalisches Institut, Georg-August-Universität Göttingen, Friedrich-Hund-Platz 1, 37077 Göttingen, Germany*

(Received 20 January 2008; revised manuscript received 2 March 2008; published 4 April 2008)

Smoothing of rough amorphous metallic surfaces by bombardment with heavy ions in the low keV regime is investigated by a combined experimental-simulation study. Vapor deposited rough amorphous  $Zr_{65}Al_{7.5}Cu_{27.5}$  films are the basis for systematic *in situ* scanning tunneling microscopy measurements on the smoothing reaction due to 3 keV  $Kr^+$  ion bombardment. The experimental results are directly compared to the predictions of a multiscale simulation approach, which incorporates stochastic rate equations of the Langevin type in combination with previously reported classical molecular dynamics simulations [Phys. Rev. B **75**, 224107 (2007)] to model surface smoothing across length and time scales. The combined approach of experiments and simulations clearly corroborates a key role of ion induced viscous flow and ballistic effects in low keV heavy ion induced smoothing of amorphous metallic surfaces at ambient temperatures.

DOI: 10.1103/PhysRevB.77.155406

PACS number(s): 61.80.Az, 61.43.Fs, 68.37.Ef, 61.43.Bn

## I. INTRODUCTION

With a strongly increasing demand for miniaturization in science and technology, controlling and manipulating surface structures have attracted interest of numerous researchers during the last decade. In this context, bombardment with heavy ions has proven to be a very versatile tool to either regularly structure surfaces (see, e.g., Refs. 1–3 for representative examples) or create ultrasmooth surfaces,<sup>4–6</sup> which are desirable in electronic and magnetic applications. A recent review on this topic is given in Ref. 7. For industrial use, ion irradiation in the low keV regime is of particular interest, since it can result in a great variety of surface structures when using a broad range of conditions—in particular, oblique incidence.<sup>1–3</sup> In ion driven systems, structure formation usually occurs as a result of the interplay of roughening and smoothing mechanisms, while the identification of the underlying physics is a long standing, yet greatly unresolved problem. The present work aims to address the physics of ion induced surface smoothing mechanisms by employing a combined experimental-simulation study using 3 keV  $Kr^+$  ion bombardment of amorphous metallic  $Zr_{65}Al_{7.5}Cu_{27.5}$  surfaces as a model system.<sup>8</sup> In fact, thin films of this glassy metallic alloy have proven to be very advantageous for quantitatively understanding growth properties<sup>9–12</sup> in the framework of kinetic roughening and self-organized structure formation. Previous studies on ion bombardment of this alloy only focused on ions in the MeV energy range,<sup>4,13</sup> where surface modification can particularly be related to thermal spike induced volume viscous flow.

In a recent work,<sup>14</sup> molecular dynamics (MD) simulations were employed to address the relative relevance of several smoothing mechanisms during keV heavy ion bombardment, among them are (i) surface diffusion, (ii) ion induced viscous flow,<sup>4,5</sup> and (iii) ballistic smoothing<sup>6</sup>—a topic that is being controversially discussed in literature (e.g., Refs. 1–7). To summarize the key tendencies for ion bombardment of an amorphous CuTi model system at ambient temperatures, we note that viscous and ballistic smoothings always overcome surface diffusion in the case of low keV ion irradiation, while

viscous flow increasingly dominates in the presence of higher energies in the MeV range and smaller lateral surface structures. In the present work, we aim to employ these findings in a numerical solution of a coarse-grained stochastic rate equation for verification in direct comparison with experiments on smoothing by low keV ion bombardment.

Before proceeding to a detailed description of the experimental and simulation methods, we first introduce basic concepts for quantifying surface structure evolution. From previous experiments,<sup>12</sup> we conclude that the surface morphology under the present conditions can be well described in the nonoverhang approximation by employing a single-valued function,  $z=h(\vec{x},t)$ , on the two dimensional substrate plane,  $\vec{x}=(x,y)$ , viz., the so-called Monge parametrization. Under this assumption, the spatiotemporal evolution of the surface in the presence of an external stochastic disturbance (i.e., ion bombardment) is described by stochastic rate equations of the Langevin type,<sup>15</sup>

$$\frac{\partial h(\vec{x},t)}{\partial t} = G[h(\vec{x},t)] + P + \xi(\vec{x},t). \quad (1)$$

Here, the functional  $G[h(\vec{x},t)]$  (usually a sum of various derivatives of  $h$  up to  $\nabla^4 h$ ) describes the modification rate of  $h$  by surface processes,  $P$  constitutes a velocity contribution by material removal, and  $\xi$  represents spatially and temporally uncorrelated Gaussian white noise due to the randomness of the processes, i.e.,

$$\langle \xi(\vec{x},t) \rangle_{\text{ensemble}} = 0, \quad (2)$$

$$\langle \xi(\vec{x},t) \xi(\vec{x}',t') \rangle_{\text{ensemble}} = 2R \delta(\vec{x} - \vec{x}') \delta(t - t'), \quad (3)$$

with the noise strength  $R$ . Employing a moving reference frame,  $P$  can be omitted after a simple coordinate transformation, as in the following. The rms roughness  $\sigma$  as well as the power spectral density can be easily calculated using (see, e.g., Ref. 15),

$$\sigma = \sqrt{\langle (\tilde{h}(\vec{x}))^2 \rangle_{\vec{x}}} \quad (4)$$

and

$$C(\vec{q}) = |\text{FT}[\tilde{h}(\vec{x})]|^2. \quad (5)$$

Here,  $\tilde{h}$  is defined by  $\tilde{h}(\vec{x}) = h(\vec{x}) - \langle h(\vec{x}) \rangle_{\vec{x}}$  and FT represents a Fourier transformation. Due to isotropy in the substrate plane, the power spectral density is usually azimuthally averaged without losing any information, resulting in  $C(q) = \langle C(\vec{q}) \rangle_{|\vec{q}|=q}$ . In fact,  $C(q)$  has proven extremely useful for an identification of surface-effective processes within a linear approximation with respect to  $h$  in the limit of large times,<sup>16</sup> based on ideas of Herring and Mullins.<sup>17,18</sup> By Fourier transforming the linear approximation of Eq. (1), we obtain

$$\frac{\partial \hat{h}(\vec{q}, t)}{\partial t} = -\hat{h}(\vec{q}, t) \sum_{i=1}^4 b_i q^i + \hat{\xi}(\vec{q}, t), \quad (6)$$

which has an exact numerical solution for the power spectral density,<sup>4,16</sup>

$$C(q, t) = C_0(q) \exp\left(-2t \sum_{i=1}^4 b_i q^i\right) + R \frac{1 - \exp(-2t \sum_{i=1}^4 b_i q^i)}{\sum_{i=1}^4 b_i q^i}, \quad (7)$$

assuming an initially rough surface [corresponding to  $C_0(q)$ ]. In the presence of smoothing mechanisms, this leads to a steady state behavior in the long-time limit,

$$C(q) = \frac{R}{\sum_{i=1}^4 b_i q^i}, \quad (8)$$

which unveils information on the magnitude of the coefficients  $b_i$ .

## II. EXPERIMENTAL DETAILS

As a paradigm to systematically address morphology evolution of amorphous surfaces in the course of bombardment with heavy ions, we choose vapor deposited glassy  $\text{Zr}_{65}\text{Al}_{7.5}\text{Cu}_{27.5}$  thin films, which are exposed to 3 keV  $\text{Kr}^+$  ions. As already detailed before,<sup>9-12</sup> rough surfaces with corrugations up to 10 nm are obtained when cocondensing 480 nm thick films with nominal rates of 0.79 nm/s from three independently rate-controlled electron beam evaporators onto  $\text{SiO}_2$  substrates using ultrahigh vacuum conditions.

Our choice of  $\text{Zr}_{65}\text{Al}_{7.5}\text{Cu}_{27.5}$  is motivated by its high stability against crystallization during exposure to elevated temperature<sup>8</sup> and ions,<sup>13</sup> which even allows us to access the supercooled liquid regime. The composition is maintained within an accuracy of  $\sim 0.5$  at % for our deposition parameters. Without breaking ultrahigh vacuum, the films are subsequently ion bombarded at room temperature by sweeping a 3 keV  $\text{Kr}^+$  ion beam, which is directed normal to the surface, across the sample.<sup>19</sup> While the ion fluence is calibrated with a Faraday cup prior to bombardment, sample currents of approximately  $0.4 \mu\text{A}/\text{cm}^2$  are kept throughout the experiments up to final fluences of  $\Phi = 4 \times 10^{17}$  ions/ $\text{cm}^2$ . When

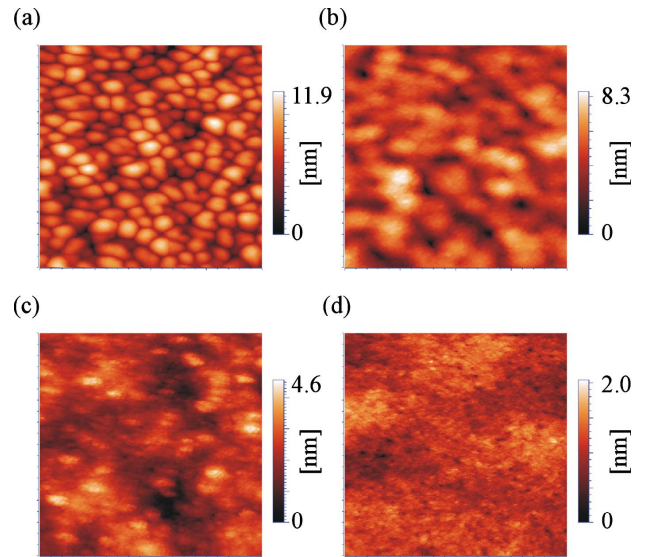


FIG. 1. (Color online) STM surface topographs of an originally 480 nm thick  $\text{Zr}_{65}\text{Al}_{7.5}\text{Cu}_{27.5}$  film (a) as grown and irradiated by 3 keV  $\text{Kr}^+$  ions with fluences of (b)  $\Phi = 7 \times 10^{15}$  ions/ $\text{cm}^2$ , (c)  $\Phi = 7 \times 10^{16}$  ions/ $\text{cm}^2$  and (d)  $\Phi = 3 \times 10^{17}$  ions/ $\text{cm}^2$  (image size: 200 nm  $\times$  200 nm).

reaching a desired fluence, the irradiation process is temporarily interrupted for surface characterization by *in situ* scanning tunneling microscopy (STM).<sup>20</sup> To address the surface topography, sample areas of 200  $\times$  200 nm<sup>2</sup> and 400  $\times$  400 nm<sup>2</sup> are scanned with electrochemically etched tungsten tips<sup>9</sup> in constant current mode ( $U = 1.0$  V;  $I = 0.8$  nA) with 400 points per line resolution. Test experiments indicated that surfaces were not critically affected by the intermittent nature of the irradiation process nor by the exact choice of the ion current within the experimentally accessible ranges. At the end of the study, amorphicity of the films is verified by *ex situ* x-ray diffraction using  $\text{Cu}_{K\alpha}$  radiation in a  $\Theta/2\Theta$  diffractometer.

## III. EXPERIMENTAL RESULTS

Figure 1 shows a selection of STM topographs, which represent major stages of morphology evolution in the course of 3 keV  $\text{Kr}^+$  ion bombardment of rough  $\text{Zr}_{65}\text{Al}_{7.5}\text{Cu}_{27.5}$  thin films. Besides the presented measurements, surfaces were characterized for a total of 14 different fluences, which all proved to be consistent with the selection of Fig. 1. Qualitatively, the mesoscopic hill-like structures of the as-grown film successively smear out and finally disappear during ion bombardment, while only weak, apparently random surface corrugations of a much larger in-plane size are observed at a fluence of  $3 \times 10^{17}$  ions/ $\text{cm}^2$ . In fact, the corrugations of as-grown films seem to coalesce during irradiation, causing the average lateral structure size to grow. In the following, we quantitatively address this scenario, i.e., the spatiotemporal evolution of surface corrugations, by calculating rms roughnesses and azimuthally averaged spectral power densities  $C(q)$ . To exclude artifacts from the limited sizes of the STM

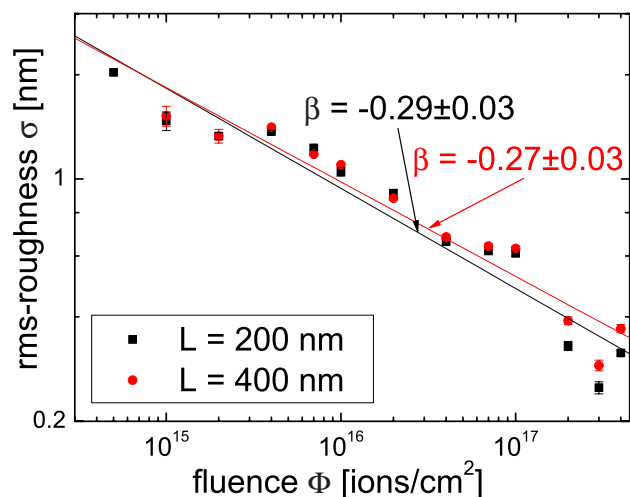


FIG. 2. (Color online) rms roughnesses as a function of ion fluence for STM topographs (edge lengths of scan areas:  $L=200$  and  $400$  nm) together with fits according to  $\sigma \propto \Phi^\beta$ .

scan areas on the one hand and the resolution of the STM raster grid on the other, we chose to analyze squared areas with two different edge lengths,  $L=200$  nm and  $L=400$  nm, with  $400 \times 400$  pixel each. As indicated by the double logarithmic plot in Fig. 2, the rms roughnesses as functions of fluence can be well described by power law scaling behavior, as expected in kinetic roughening and/or smoothing scenarios.<sup>15</sup> For all fluences investigated,  $C(q)$  has been calculated and plotted on a double logarithmic scale to obtain the signatures of the dominant processes in linear approximation (Sec. I). However, to keep the graph in Fig. 3 concise, we decided to restrict ourselves here only to representative fluences, which correspond to the main stages of structure evolution. In the range of large enough wave vectors  $q$ , where  $C(q)$  is expected to reach its steady state, the data are well fitted by a power law,  $C(q) \propto q^{-\zeta}$ , as expected. During ion bombardment, the exponent  $\zeta$  decreases from  $\zeta$

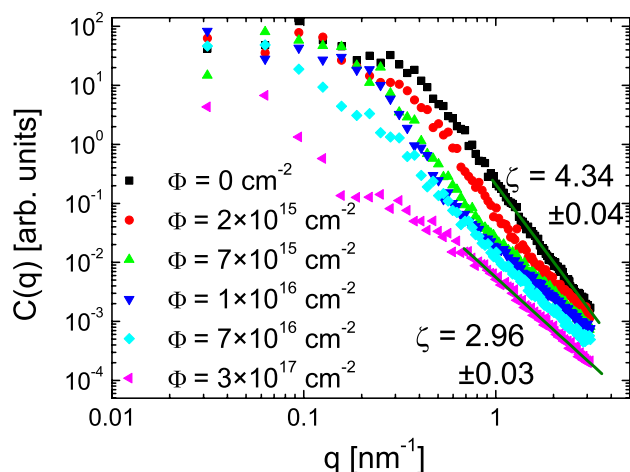


FIG. 3. (Color online) Power spectral densities as calculated for STM topographs (Fig. 1) together with fits according to a power law of  $C(q) \propto q^{-\zeta}$ .

$= 4.34 \pm 0.04$  (for the as prepared film) to  $\zeta = 2.96 \pm 0.03$  (for the surface with the highest ion induced smoothness). A fit of the power spectral densities according to Eq. (7) yields dominating processes with  $q$  to the power of 2 and 4 for the smooth surface.<sup>21</sup> In fact, both corresponding processes are smoothing processes due to their respective algebraic signs. The latter scenario is accompanied by a decrease in the intensity of  $C(q)$ , which most strongly appears for those wave vectors which correspond to the dominating structure size of the as-grown film. Thus, this finding quantitatively confirms that ion induced film smoothing primarily proceeds by successive elimination of the dominant surface modulations—successively from smaller to larger length scales.

#### IV. MULTISCALE MODELING OF SURFACE SMOOTHING

Ion bombardment induced surface modification clearly occurs on multiple length and time scales, consequently requiring a multiscale simulation approach: While the size and lifetime of an individual collision cascade (some nanometers and picoseconds, respectively) need to be addressed by atomistic simulations, mesoscopic structure formation on experimental time scales (microns and tens of minutes) requires a coarse-grained model, which incorporates the atomistic processes in an averaged or effective way. In the present work, this is achieved by linking classical molecular dynamics simulations with empirical potentials<sup>14</sup> to a continuum description in the framework of stochastic rate equations of surface evolution. While both concepts for themselves are well established in literature,<sup>15,22</sup> systematic linkages have hardly been performed (see Ref. 6 for a recent example).

For the case of film growth from vapor, we have shown in previous publications<sup>9–11</sup> that experimental topographies and their evolutions are well described by stochastic rate equations, assuming (i) surface diffusion, (ii) self-shadowing, and (iii) overgrowth as dominant processes. We use this simulated morphology for a  $480$  nm thick film as a starting point for the present studies in the following. Upon bombardment with heavy energetic ions in the low keV regime, surface smoothing is predominantly governed by surface viscous flow<sup>23,5</sup> and ballistic effects,<sup>6</sup> as also corroborated by the analyses of the experimental power spectral densities (processes with  $q^2$  and  $q^4$ —see Sec. III), yielding

$$\frac{\partial h(\vec{x}, t)}{\partial t} = c_1 \nabla^2 h + c_2 \nabla^4 h + \xi(\vec{x}, t). \quad (9)$$

Both deterministic terms on the right hand side represent smoothing terms with coefficients  $c_1 > 0$  and  $c_2 < 0$ —in accordance with the fit of the experimental power spectra in Sec. III. Expressions which relate  $c_1$  and  $c_2$  to materials and/or physical properties, as well as a quantitative estimate for their ratio, have been derived in Ref. 14. The resulting expressions for the coefficients read

$$c_1 = \left| \frac{F\Omega\delta}{\tan(\alpha)} \right|, \quad (10)$$

TABLE I. Parametrization of Eq. (9).

$c_1$ [nm <sup>2</sup> /(ions/cm <sup>2</sup> )]	$c_2$ [nm <sup>4</sup> /(ions/cm <sup>2</sup> )]	$R$ [nm <sup>4</sup> /(ions/cm <sup>2</sup> )]
$3.224 \times 10^{-15}$	$-3.24 \times 10^{-13}$	$2.152 \times 10^{-17}$

$$c_2 = -\frac{\gamma a_z^3}{3\eta}, \quad (11)$$

where  $\gamma$ ,  $\eta$ ,  $a_z$ ,  $\Omega$ , and  $F$  denote the surface free energy, the radiation induced viscosity, the average out of plane size of a thermal spike, the average atomic volume, and the flux of incoming ions, respectively. If ions hit the surface under off-normal incidence,  $\alpha$  is the angle of inclination and  $\delta$  describes the sum of ballistic atomic lateral displacements. In Ref. 14, we identified a transition from a viscous flow to a ballistic displacement dominated regime of surface smoothing, where the lateral size of the surface corrugations, viz., its dominant wavelength  $\lambda$ , turned out to be the decisive quantity. With the corresponding crossover wavelength between both regimes,

$$\lambda_c = 2\pi \sqrt{\left| \frac{\gamma a_z^3 \tan(\alpha)}{3\eta F \Omega \delta} \right|}, \quad (12)$$

the relation between both coefficients,  $c_1$  and  $c_2$ , is readily expressed as

$$c_2 = -\left(\frac{\lambda_c}{2\pi}\right)^2 c_1. \quad (13)$$

In the range of low keV ion bombardment with an effective sputter yield  $Y$ , the noise strength induced by sputtering is given by<sup>4,15,24</sup>

$$2R = FY\Omega^2. \quad (14)$$

In combination with Eq. (10), this results in the following relation between  $R$  and  $c_1$ :

$$c_1 = \frac{2R \left| \frac{\delta}{\tan(\alpha)} \right|}{Y\Omega}. \quad (15)$$

With Eqs. (13)–(15) and the results of previous MD simulations,<sup>14</sup> it is possible to estimate all parameters, which appear in Eq. (9). We would like to note that the flux of incoming ions  $F$  is represented by the value of our experimental studies, while the sputter yield is additionally estimated from MD simulations. As we have observed the production of adatoms (i.e., loosely bound, highly mobile atoms on the surface) in the MD simulations,<sup>14</sup> it is reasonable to assume that adatoms additionally induce a noisy roughness on the atomistic scale similar to that of sputter erosion. Therefore,  $Y$  will be assumed to be given by the sum of sputtered atoms and adatoms produced per incoming ion in the following. Taking this into account, the parameters for the equation describing surface structure evolution are calculated and listed in Table I.

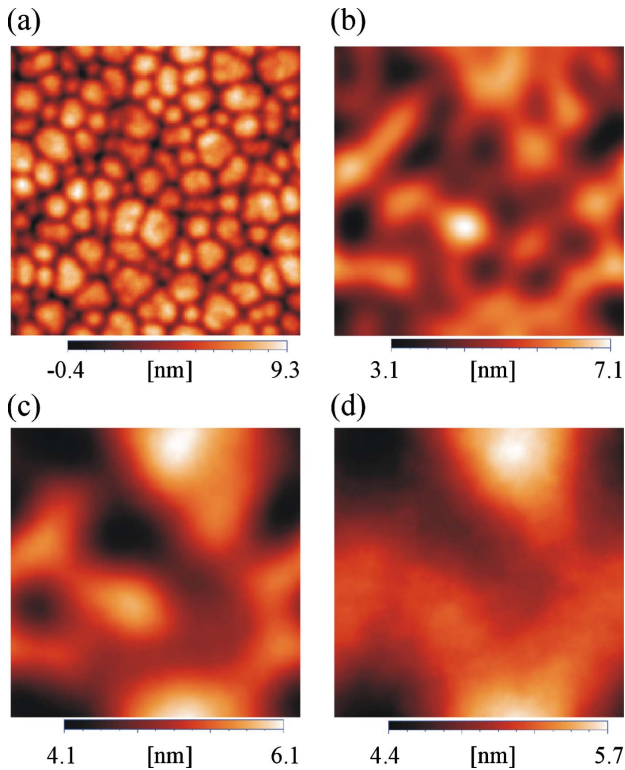


FIG. 4. (Color online) Surface topographs from continuum model simulations for representative ion fluences following Eq. (9) and Table I. (a) Starting point is a simulated 480 nm thick vapor deposited  $Zr_{65}Al_{7.5}Cu_{27.5}$  film (Refs. 9 and 10), which subsequently shows a [(b)–(d)] smoothing reaction as a function of fluence: (a)  $\Phi=0$  ions/cm<sup>2</sup>, (b)  $\Phi=2.5 \times 10^{15}$  ions/cm<sup>2</sup>, (c)  $\Phi=1.5 \times 10^{16}$  ions/cm<sup>2</sup>, and (d)  $\Phi=7.5 \times 10^{16}$  ions/cm<sup>2</sup> (image sizes of  $200 \times 200$  nm<sup>2</sup>).

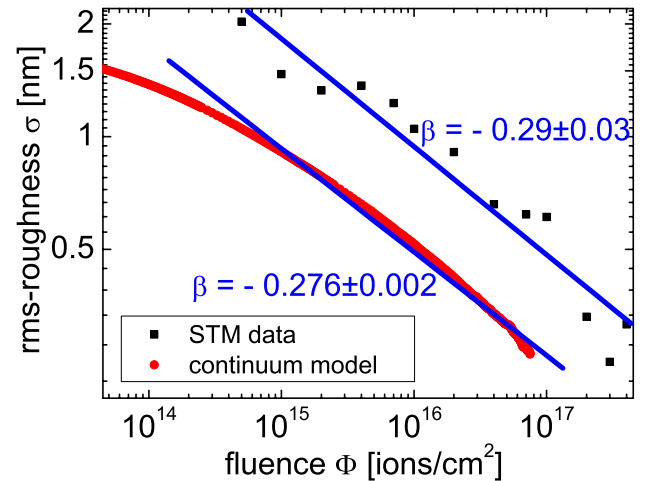


FIG. 5. (Color online) rms roughnesses as a function of fluence for continuum model simulations and STM data (image sizes  $200 \times 200$  nm<sup>2</sup>) with a fit according to  $\sigma \propto t^\beta$ .

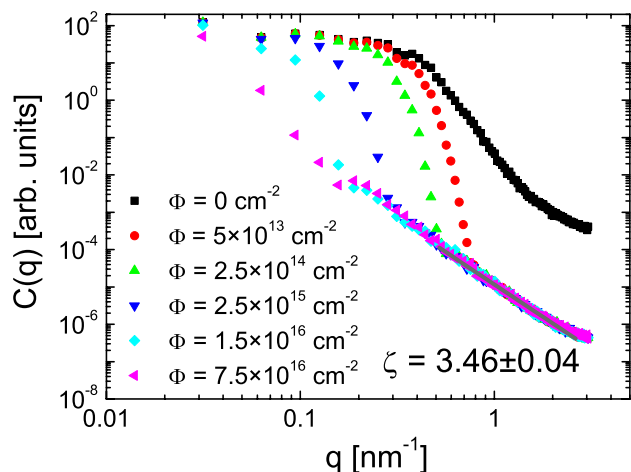


FIG. 6. (Color online) Power spectral densities as extracted from the numerical solution of the continuum model; results for several fluences are presented together with fits according to a power law of  $C(q) \propto q^{-\zeta}$ .

## V. MODELING RESULTS

Starting from a simulated<sup>9–11</sup> 480 nm thick  $\text{Zr}_{65}\text{Al}_{7.5}\text{Cu}_{27.5}$  film on  $\text{SiO}_2$ , the ion induced surface smoothing reaction is modeled by solving Eq. (9) with the parametrization of Table I. This is numerically achieved by discretization in space (using a square  $200 \times 200 \text{ nm}^2$  grid with a spatial resolution of 1 nm and periodic boundaries in the substrate plane) and application of the Euler scheme for temporal integration (time step  $\Delta t = 0.001 \text{ s}$ ), which has proven to supply reliable solutions in previous systematic studies.<sup>9</sup> The evolution of surface structures (Fig. 4) qualitatively reveals reasonable consistency with the experimental results (Fig. 1): The surface smoothens and the lateral structure size increases. The corresponding rms roughnesses are plotted in Fig. 5 together with the experimental data observed for the same image size on double-logarithmic scales. We would like to note that we choose the ion fluence as the intrinsic time scale of our studies, which is proportional to the time  $t$  in the continuum model with the ion flux being the proportionality factor. We find a power law behavior in the continuum model with an exponent close to its experimental counterpart. In Fig. 6, the power spectral densities for representative stages in the evolution of the continuum model are presented. The decay of  $C(q)$  in the range of large  $q$  values changes from a  $q^{-4}$  behavior (as observed for film growth) to a  $q^{-\zeta}$  behavior with  $\zeta = 3.46 \pm 0.04$ .

## VI. DISCUSSION

From Figs. 1–6, it becomes clear that the basic features of the experimental observations can be reproduced by the present continuum model. This is particularly true for the evolution of the rms roughnesses in experiments and simulations, which exhibit power law decays with almost identical exponents  $\beta$ . As for the power spectral densities, we observe transitions to a less steep decay for large  $q$  values, when comparing as-grown films with their irradiated coun-

terparts in experiments and simulations. Compared to the experiments, the decay remains slightly steeper in the continuum model. In fact, quantitative differences between experiments and simulations are not too surprising, as the coefficients of the continuum model were based on MD simulations on a  $\text{Cu}_{50}\text{Ti}_{50}$  model glass due to availability of a reliable potential, while the experiments had to be performed on  $\text{Zr}_{65}\text{Al}_{7.5}\text{Cu}_{27.5}$  to prevent crystallization. Although  $\text{Cu}_{50}\text{Ti}_{50}$  and  $\text{Zr}_{65}\text{Al}_{7.5}\text{Cu}_{27.5}$  surely share a lot of common features (note particularly the close chemical similarity of Ti and Zr), the unresolved impact of the Al content in glassy dynamics<sup>25</sup> and the absence of covalent bonds in the embedded atom method description of CuTi surely constitute deficiencies, which may well explain reduced roughnesses or, similarly, lower effective ion fluences for simulations in Fig. 5. While consequently rescaling must be an integral part of any quantitative comparison of quantities, such as fluence, roughness, or power spectral density, the excellent agreement in terms of scaling behavior is a strong indication of a correct incorporation of the significant physics in the present model description. In the following, we therefore focus on the scaling exponents—of rms roughness and power spectral densities—and their implications, in particular.

We first note that a tight relationship exists between the scaling behavior of roughnesses and power spectral density: The power law behavior of the rms roughness can be concluded from the relation between roughness and power spectral density,  $(\sigma(t))^2 = \int C(\vec{q}, t) d\vec{q}$ , and Eq. (7). Assuming  $C_0(q) = \text{const}$  leads to smoothing of the original structures according to  $\sigma(t) \propto t^{-1/i}$  if the dominating smoothing mechanism corresponds to  $C(q) \propto q^{-i}$ .<sup>21</sup> As presently we are dealing with a combination of smoothing processes primarily with  $i=2$  and  $i=4$ , we observe a power law decay of the rms roughness  $\sigma(t) \propto t^\beta$ , with  $-1/2 < \beta < -1/4$ . The effective exponent  $\zeta$  in a fit according to  $C(q) \propto q^{-\zeta}$ , on the other hand, is strongly related to dominant surface processes according to Eq. (8). The fact that  $\zeta$  exhibits larger values in the continuum model when compared to the experiment can be explained by the following argument: For the case of low keV ion bombardment, the thickness of the surface layer, in which viscous flow due to thermal spikes prevails, is small compared to the structure size of the irradiated surface. Therefore, smoothing due to viscous flow is basically represented by surface viscous flow in the present model,<sup>23</sup> viz. a  $\nabla^4 h$  term in Eq. (9). Clearly, this process enters the power spectral densities with a  $q^{-4}$  term. If the thickness of the liquid layer is, however, larger than the structure size, viscous smoothing would be governed by volume viscous flow and enter the power spectral densities with a  $q^{-1}$  term.<sup>4</sup> More realistically, the overall flow process therefore should possibly be described by a superposition of volume and surface viscous flow. In fact, if a small contribution to the overall flow is contributed by volume viscous flow, a smaller value of  $\zeta$ —when compared to a pure surface process—should be expected. Thus, the small deviation of  $\zeta$  in experiments and simulations presumably indicates a small portion of volume viscous flow in the total viscous flow process in addition to the overall dominating surface viscous flow.

Additionally, in the course of this work, we have investigated<sup>21</sup> a continuum model for ion irradiation with

$c_1 < 0$  and  $c_2 < 0$ , which mathematically corresponds to a Bradley–Harper-type model.<sup>26</sup> The latter results in exponents  $\beta$  and  $\zeta$  with smaller and larger absolute values, respectively, than the experiments and our continuum model. As an enhancement of the smoothing  $\nabla^4 h$  term would even increase  $\zeta$ , while a stronger roughening  $\nabla^2 h$  term would decrease the absolute value of  $\beta$ , a Bradley–Harper-type model clearly leads to less agreement with the present experiments.

## VII. CONCLUSIONS

In conclusion, we have shown that a structured amorphous surface can be smoothed by ion bombardment in the low keV energy range. Additionally, we presented a minimum continuum model, which is numerically solved. It ex-

hibits agreement with the experimental results with regard to the essential characteristics. The results from experiments and continuum modeling corroborate the idea that surface viscous flow and ballistic smoothing are constitutive mechanisms during low keV ion bombardment under normal incidence on structured amorphous surfaces at ambient temperatures. Future research in this field might include further—particularly higher-order—extensions to the present minimum model.

## ACKNOWLEDGMENTS

We acknowledge the Gesellschaft für Wissenschaftliche Datenverarbeitung Göttingen, Germany (GWDG) for a grant of computing time and the German DFG (SFB 602 TP B3) for funding.

\*svauth@gwdg.de

†smayr@gwdg.de

<sup>1</sup>T. M. Mayer, E. Chason, and A. J. Howard, *J. Appl. Phys.* **76**, 1633 (1994).

<sup>2</sup>F. Frost, A. Schindler, and F. Bigl, *Phys. Rev. Lett.* **85**, 4116 (2000).

<sup>3</sup>J. Erlebacher, M. J. Aziz, E. Chason, M. B. Sinclair, and J. A. Floro, *Phys. Rev. Lett.* **82**, 2330 (1999).

<sup>4</sup>S. G. Mayr and R. S. Averback, *Phys. Rev. Lett.* **87**, 196106 (2001).

<sup>5</sup>C. C. Umbach, R. L. Headrick, and K.-C. Chang, *Phys. Rev. Lett.* **87**, 246104 (2001).

<sup>6</sup>M. Moseler, P. Gumbsch, C. Casiraghi, A. C. Ferrari, and J. Robertson, *Science* **309**, 1545 (2005).

<sup>7</sup>W. L. Chan and E. Chason, *J. Appl. Phys.* **101**, 121301 (2007).

<sup>8</sup>A. Inoue, D. Kawase, A. P. Tsai, T. Zhang, and T. Matsumoto, *Mater. Sci. Eng., A* **178**, 255 (1994).

<sup>9</sup>S. G. Mayr, M. Moske, and K. Samwer, *Phys. Rev. B* **60**, 16950 (1999).

<sup>10</sup>M. Raible, S. G. Mayr, S. J. Linz, M. Moske, P. Hänggi, and K. Samwer, *Europhys. Lett.* **50**, 61 (2000).

<sup>11</sup>C. Streng, K. Samwer, and S. G. Mayr, *Appl. Phys. Lett.* **81**, 5135 (2002).

<sup>12</sup>S. Vauth, C. Streng, S. G. Mayr, and K. Samwer, *Phys. Rev. B* **68**, 205425 (2003).

<sup>13</sup>S. G. Mayr, *J. Appl. Phys.* **97**, 096103 (2005).

<sup>14</sup>S. Vauth and S. G. Mayr, *Phys. Rev. B* **75**, 224107 (2007).

<sup>15</sup>For an overview and further references, see, e.g., A.-L. Barabasi and H. E. Stanley, *Fractal Concepts in Surface Growth* (Cambridge University Press, Cambridge, UK, 1995).

<sup>16</sup>J. Villain, *J. Phys. I* **1**, 19 (1991).

<sup>17</sup>C. Herring, *J. Appl. Phys.* **21**, 301 (1950).

<sup>18</sup>W. W. Mullins, *J. Appl. Phys.* **30**, 77 (1959).

<sup>19</sup>Varian Ion Bombardment Gun, Model 981-2043, a commercial sputtering gun.

<sup>20</sup>Omicron STM 1, scanning tunneling microscope.

<sup>21</sup>S. Vauth, Ph.D. thesis, Göttingen, 2007.

<sup>22</sup>M. P. Allen and D. J. Tildesley, *Computer Simulation of Liquids* (Clarendon, Oxford, UK, 1987).

<sup>23</sup>S. E. Orchard, *Appl. Sci. Res., Sect. A* **11**, 451 (1962).

<sup>24</sup>S. F. Edwards and D. R. Wilkinson, *Proc. R. Soc. London, Ser. A* **381**, 17 (1982).

<sup>25</sup>M. Guerdane and H. Teichler, *Phys. Rev. B* **65**, 014203 (2001).

<sup>26</sup>R. M. Bradley and J. M. E. Harper, *J. Vac. Sci. Technol. A* **6**, 2390 (1988).